

Correlations of modulation noise with magnetic microstructure and intergranular interactions for CoCrTa and CoNi thin-film media

Mahbub R. Khan, S. Y. Lee, S. L. Duan, J. L. Pressesky, and Neil Heiman
Seagate Magnetics, 47001 Benicia Street, Fremont, California 94538

Dennis E. Speliotis
Advanced Development Corporation, 8 Ray Avenue, Burlington, Massachusetts 01803

M. R. Scheinfein
National Institute of Standards and Technology, Gaithersburg, Maryland 20899

This paper reports on two thin-film media alloys $\text{Co}_{86}\text{Cr}_{12}\text{Ta}_2$ and $\text{Co}_{75}\text{Ni}_{25}$ which have very different noise characteristics. The magnetic microstructure of these films was observed with scanning electron microscopy with polarization analysis (SEMPA). The variance (σ_t^2) of the magnetization across the transition region was calculated. The origin of anisotropy was determined by measuring the temperature coefficients of H_c and M_s . The interaction strengths between grains, $\delta M(H)$, were obtained from the measurements of the reverse demagnetization remanence $M_d(H)$ and the forward magnetization remanence $M_r(H)$. We found that the CoNi film showed a greater degree of interparticle interaction, which may explain the observed cross-bit linkages in SEMPA image, larger rms transition variation (σ_t), and higher modulation noise.

INTRODUCTION

Recently, there has been much interest in the noise characteristics of recording media¹⁻⁴ which have not been completely explained by current theoretical models.^{1,4-8} There are reports of noise correlations with anisotropy constant K ,^{4,6} grain-boundary segregation and magneto-static or exchange interactions,^{4,7} coercive squareness S^* ,⁸ rotational hysteresis integral Rh ,⁴ irregularities of zigzag transitions,^{3,4} etc. This paper reports on CoCrTa and CoNi samples which have very different noise characteristics.^{2,4} The magnetic microstructure using scanning electron microscopy with polarization analysis⁹ (SEMPA) and anisotropy of these two alloys have been reported elsewhere.⁴ Additional studies were carried out on these two samples to determine the origin of anisotropy, make measurements of interactions between grains, and calculate the variance (σ_t^2) of the magnetization across the transition region.

Wohlfarth¹⁰ showed that

$$M_d(H) = M_r(\infty) - 2M_r(H), \quad (1)$$

under the assumption of uniaxial anisotropy, no particle interactions, no superparamagnetic, multidomain, or incoherent rotation effects. Here, $M_r(H)$ is the forward magnetization remanence and $M_d(H)$ is the reverse demagnetization remanence. $M_r(H)$ is obtained by forward application and subsequent removal of H . $M_d(H)$ is acquired after dc saturation in forward direction and the subsequent application and removal of H in the reverse direction. Kelly, O'Grady, and Chantrell¹¹ normalized Wohlfarth's equation and added an interaction term $\delta M(H)$ as follows:

$$M_d(H)/M_r(\infty) = 1 - 2M_r(H)/M_r(\infty) + \delta M(H). \quad (2)$$

$\delta M(H)$ can also be expressed as

$$\delta M(H) = 2(P_r - P_d). \quad (3)$$

Here, P_r and P_d are the fraction of crystallites switched at a field H in $M_r(H)$ mode and $M_d(H)$ mode, respectively, and are defined as $P_r = M_r(H)/M_r(\infty)$ and $P_d = 0.5 [1 - M_d(H)/M_r(\infty)]$. The intergranular interactions $\delta M(H)$ are obtained from the measured values of $M_d(H)$ and $M_r(H)$.

EXPERIMENTAL PROCEDURE

The $\text{Co}_{86}\text{Cr}_{12}\text{Ta}_2$ and $\text{Co}_{75}\text{Ni}_{25}$ samples were prepared by dc magnetron sputtering with a 400-Å-thick Cr underlayer on circumferentially textured 95-mm NiP/Al substrates.

The magnetic properties of these films were measured with a vibrating-sample magnetometer (VSM). The read-back noise measurements were made with a minimonolithic 3370 slider-type Winchester recording head with a gap width of 40 μin . and a flying height of 16 μin .^{2,4} The integrated noise voltage was determined by sampling the noise spectrum at 0.25-MHz intervals over a bandwidth of 10 MHz. The writing frequency ranged from 2.5 to 12.5 MHz at the optimum write current of 20-mA 0- p (zero to peak).

TABLE I. Magnetic and recording properties of $\text{Co}_{86}\text{Cr}_{12}\text{Ta}_2$ and $\text{Co}_{75}\text{Ni}_{25}$ films.

	CoCrTa	CoNi
Thickness (μm)	0.07	0.043
M_s (emu/cm ³)	660	1070
H_c (Oe)	693	730
M_r (memu/cm ²)	3.80	4.02
S	0.820	0.874
S^*	0.893	0.903
E_0 0- p (μV)	342	365
T_{50} (ns)	206	204

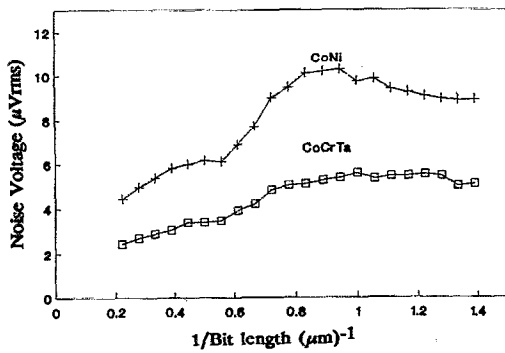


FIG. 1. Noise voltage vs recording densities for $\text{Co}_{86}\text{Cr}_{12}\text{Ta}_2$ and $\text{Co}_{75}\text{Ni}_{25}$ films. SEMPA samples were written at $0.588 (\mu\text{m})^{-1}$.

The magnetic microstructure of these films was observed using SEMPA.^{4,9} The SEMPA samples were prepared by writing with 20-mA 0-p (zero-to-peak) write current on a dc-erased surface with bit density of 588 fc/mm.

The rms variation of the magnetization across the transition as observed on the SEMPA images was calculated as follows: First, the transition was digitized in the x - y plane. Then, the average coordinate of the transition (\bar{Y}) was determined from $\bar{Y} = 1/N \sum_{i=1}^N y_i(x_i)$ and the variance (σ_i^2) was calculated as

$$\sigma_i^2 = 1/(N-1) \sum_{i=1}^N [y_i(x_i) - \bar{Y}]^2, \quad (4)$$

$$\text{rms}(\sigma_i) = \sqrt{\sigma_i^2}.$$

The temperature coefficients of coercivity H_c and saturation magnetization M_s were determined by measuring the H_c and M_s values at different temperatures in the range -30 – 60°C using a VSM with a variable temperature attachment.

Both remanence curves $M_d(H)$ and $M_r(H)$ were measured by VSM following the procedure described above. The interaction $\delta M(H)$ were obtained for both samples using Eqs. (2) and (3).

RESULTS AND DISCUSSIONS

The magnetic properties (M_s , H_c , S , and S^*) and the recording properties (E_0 , T_{50}) of CoCrTa and CoNi samples were chosen to be nearly the same, and the results are shown in Table I.

The integrated noise voltage as a function of recording density for the optimum write current of 20-mA 0-p is



FIG. 2. SEMPA images of (a) $\text{Co}_{86}\text{Cr}_{12}\text{Ta}_2$ and (b) $\text{Co}_{75}\text{Ni}_{25}$ films. The images are of the magnetization component along the track.

TABLE II. $\text{rms}(\sigma_i)$, noise, and $\delta M(H)$ for CoCrTa and CoNi.

	$\sigma_i (\mu\text{m})$	Noise (μV)	$\delta M(H)_{\text{max}}$
CoCrTa	0.370	3.5	0.80
CoNi	0.743	6.5	1.25

shown in Fig. 1 for CoCrTa and CoNi samples. It is obvious that of the two alloys the CoNi has significantly higher noise. It also shows the onset of a superlinear increase in noise¹ for CoNi at about the density where SEMPA samples were written. CoCrTa samples do not show any clear evidence of superlinear noise behavior.

The SEMPA images of the written domains or bits in the CoCrTa and CoNi films are shown in Fig. 2. The average bit spacing is about $1.7 \mu\text{m}$. In these SEMPA images, the component of magnetization along the tracks is imaged. White (black) represents magnetization pointing forward (back) along the track in the plane of the figure. The written domains or bits for the CoCrTa sample are well separated by jagged boundaries. For CoNi specimen, the bits are cross-linked, and the neighboring domains are bridged together. The variance (σ_i^2) of the transition region was calculated by digitizing the magnetization in the x - y plane. The calculated values of rms variations (σ_i) for CoCrTa and CoNi samples are shown in Table II along with the noise data. Here, we see that σ_i is about twice as large for CoNi than CoCrTa and correlates very well with integrated noise voltage which is also about twice as large (Fig. 1) for CoNi at this density and write current.

Figure 3 shows the variation of M_s and H_c as a function of temperature with coefficients at $0.030\%/^\circ\text{C}$ and $0.24\%/^\circ\text{C}$, respectively, for CoCrTa, and $0.014\%/^\circ\text{C}$ and $0.16\%/^\circ\text{C}$, respectively, for CoNi. From the relations $H_c \propto N_d M_s$ and $H_c \propto K/M_s$, where N_d is the demagnetizing factor (related to shape), and K is the crystalline anisotropy constant, one would expect similar temperature coefficients of H_c and M_s for shape anisotropy. But the H_c temperature coefficient is about ten times larger than that of M_s . This indicates that the main contribution to H_c is crystalline anisotropy and not shape anisotropy. It is possible that stress also plays a role here and is being investigated. The thermal coefficients of CoNi are smaller than

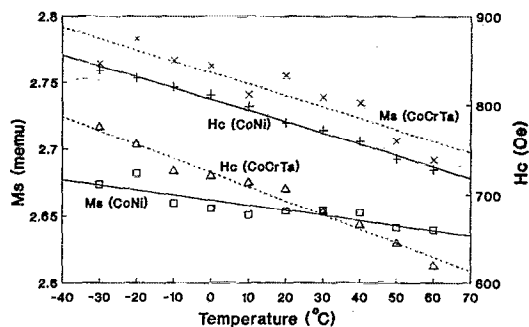


FIG. 3. M_s and H_c vs temperature for (a) CoCrTa and (b) CoNi.

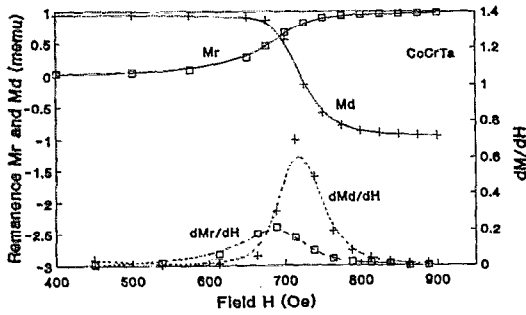


FIG. 4. $M_d(H)$ and $M_r(H)$ and the derivatives vs H for CoCrTa.

those of CoCrTa, indicating higher Curie temperature for CoNi.

Figure 4 shows $M_r(H)$ and $M_d(H)$ and the derivatives as a function of H for CoCrTa. The switching field distribution (SFD) or full width at half height (FWHH) of dM_r/dH is broader than dM_d/dH , and the peak is lower and appears at a lower field, as expected. Here, $dM_r/dH = \chi^{irr}$, the irreversible susceptibility. CoNi shows similar behavior.

Figure 5 shows the Henkel plot¹² of $M_d(H)$ vs $M_r(H)$ for CoCrTa and CoNi samples. Here, we see that the CoNi graph deviates further from the Wohlfarth line (straight) than CoCrTa, indicating stronger interactions among CoNi grains.

Figure 6 is a plot of $\delta M(H)$ vs H for both samples.¹¹ Here, we see the general trend that $\delta M(H)$ increases to a peak around the coercivity, then decreases rapidly as the value of H increases. We also clearly see that the $\delta M(H)$ peak is more than 50% higher for CoNi than CoCrTa (Table II). Therefore, the interactions between the grains of CoNi film are stronger than CoCrTa and correlates well with noise data.

CONCLUSIONS

Our CoNi sample shows higher modulation noise than CoCrTa. CoNi sample shows superlinear noise behavior as opposed to CoCrTa.

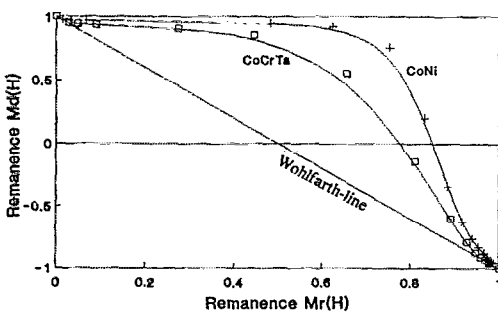


FIG. 5. Henkel plot of $M_d(H)$ vs $M_r(H)$ for CoCrTa and CoNi.

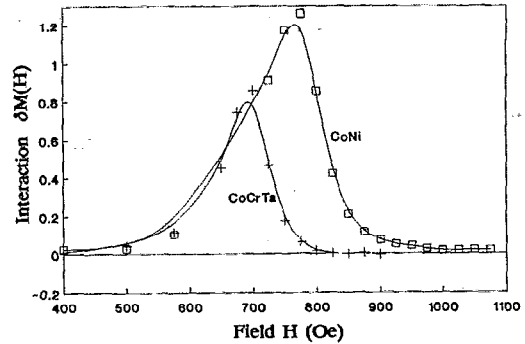


FIG. 6. Plot of $\delta M(H)$ vs H for CoCrTa and CoNi samples.

The SEMPA images show that CoCrTa domains or bits are well separated by jagged boundaries, whereas CoNi bits are cross-linked and neighboring bits are bridged together.

We did the first analysis ever of recording transitions, based on SEMPA images, where the calculations are done with the actual magnetization transition positions across the transition region written on a real sample. The results of those calculations show that the rms transition variation (σ_t) is twice as large for CoNi than CoCrTa and correlates very well with integrated noise voltage which is about twice as large for CoNi. Noise also correlates well with $\delta M(H)$.

The temperature coefficients of H_c are about ten times larger than that of M_s , and this indicates that the main contribution to H_c is crystalline anisotropy and not shape anisotropy.

¹ N. Belk, P. George, and G. Mowry, IEEE Trans. Magn. **MAG-21**, 1350 (1985).

² S. Y. Lee, J. Pressesky, D. Williams, and N. Heiman, IEEE Trans. Magn. **MAG-26**, 121 (1990).

³ H. Aoi, Y. Shiroishi, and H. Matsuyama, IEEE Trans. Magn. **MAG-24**, 2715 (1988).

⁴ M. R. Khan, S. Lee, J. Pressesky, D. Williams, S. Duan, R. Fisher, N. Heiman, M. Scheinfein, J. Unguris, D. Pierce, R. Celotta, and D. Spiliotis, IEEE Trans. Magn. **MAG-26**, 2715 (1990).

⁵ A. M. Barany and H. N. Bertram, IEEE Trans. Magn. **MAG-23**, 1776 (1987).

⁶ Y. Shiroishi, Y. Matsuda, K. Yoshida, H. Suzuki, T. Ohno, N. Tsumita, M. Ohura, and M. Hayashi, IEEE Trans. Magn. **MAG-24**, 2730 (1988).

⁷ T. Chen and T. Yamashita, IEEE Trans. Magn. **MAG-24**, 2700 (1988).

⁸ B. R. Natarajan and E. S. Murdock, IEEE Trans. Magn. **MAG-24**, 2724 (1988).

⁹ M. R. Scheinfein, J. Unguris, M. Kelley, D. Pierce, and R. Celotta, Rev. Sci. Instrum. **61**, 2501 (1990).

¹⁰ E. P. Wohlfarth, J. Appl. Phys. **29**, 595 (1958).

¹¹ P. E. Kelly, K. O'Grady, and R. Chantrell, IEEE Trans. Magn. **MAG-25**, 3881 (1989).

¹² O. Henkel, Phys. Status Solidi **7**, 919 (1964).